Solvent Effects on the Reaction Coordinate of the Hydrolysis of Phosphates and Sulfates: Application of Hammond and Anti-Hammond Postulates to Understand Hydrolysis in Solution

Xabier Lopez,[†,‡,§] Annick Dejaegere,[||] and Martin Karplus*[,‡,§,⊥]

Contribution from the Kimika Fakultatea, Euskal Herriko Unibertsitatea, P.K.1072, 20080 Donostia, Spain, Laboratoire de Chimie Biophysique, Institut le Bel, Université Louis Pasteur, 67000 Strasbourg, France, Oxford Centre for Molecular Sciences, New Chemistry Laboratory, South Parks Road, Oxford OX1 3QZ, United Kingdom, Laboratoire de Biologie et Génomique Structurales, Ecole Supérieure de Biotechnologie de Strasbourg, 67400 Illkirch, France, Department of Chemistry and Chemical Biology, Harvard University, Cambridge, Massachusetts 02138

Received March 14, 2001. Revised Manuscript Received June 28, 2001

Abstract: The mechanism of the alkaline hydrolysis of phosphate and sulfate esters is of great interest. Ab initio quantum mechanical calculations and dielectric continuum methods are used to investigate the effect of the solvent on the associative/dissociative and the in-line/sideways character of the hydrolysis reaction of ethylene sulfate (ES) and ethylene phosphate (EP^-), and their acyclic counterparts, dimethyl sulfate (DMS) and dimethyl phosphate (DMP^-). The gas-phase reaction coordinates are determined by Hartree−Fock and density functional theory. For ES, the reaction coordinate in solution is determined; for the other three reactions only the transition state in solution is obtained. The alterations in the reaction induced by solvent are interpreted by use of the Hammond and anti-Hammond postulates.

1. Introduction

The alkaline hydrolysis of phosphate and sulfate esters has been the subject of numerous experimental and theoretical studies over many years.[1−4] One reason for their interest is that these reactions are central to important biochemical processes.[5−7] To understand the underlying interactions involved, hydrolysis of phosphate and sulfate esters have been treated by high level ab initio methods,[2,3,8−17] as well as semiempirical methods.[18−20] It has been established that the rate-limiting step corresponds to the attack of the hydroxyl group on the phosphate/sulfate. The gas-phase transition state is "early" in that the X−OH distance is long, particularly relative to the X−O leaving group distance (X = P, S). The essential role of solvent in these reactions has been demonstrated,[9,13,20] in that the barrier heights are strongly influenced by the dielectric shielding. High dielectric constant solvents, such as water, lower the activation barrier with respect to the gas phase if two ionic species are involved, as for OH^- and anionic phosphates.[9,13] By contrast, solvent increases the barriers relative to the gas phase for reactions that involve the approach of one negative charge to a neutral system; examples are the attack of OH^- on neutral sulfate esters[2−4] and phosphate esters[10,11,14,21] and the attack of water or methanol on anionic phosphates.[22] On the basis of such analysis, the solvent effect has been shown to be the primary factor in the rate acceleration of the alkaline hydrolysis of cyclic phosphates/sulfates with respect to their acyclic counterparts.[4,9,13]

Solvation also influences the geometries of the transition states formed during the reaction. Lim et al.[21] determined the solvent effect on the geometry of the transition states for the hydrolysis of methyl ethylene phosphate (MEP) and its acyclic analogue, trimethyl phosphate (TMP). However, the influence of solvation on the transition-state structures differs in magnitude

[†] Euskal Herriko Unibertsitatea.
[‡] Université Louis Pasteur.
[§] Oxford Centre for Molecular Sciences.
[||] Ecole Supérieure de Biotechnologie de Strasbourg.
[⊥] Harvard University.

(1) Perreault, D. M.; Anslyn, E. V. *Angew. Chem., Int. Ed. Engl.* **1997**, *36*, 432−450.
(2) Thatcher, G.; Cameron, D. *J. Chem. Soc., Perkin Trans. 2* **1996**, 767.
(3) Cameron, D.; Thatcher, G. *J. Org. Chem.* **1996**, *61*, 5986−5997.
(4) Lopez, X.; Dejaegere, A.; Karplus, M. *J. Am. Chem. Soc.* **1999**, *121*, 5548−5558.
(5) Stote, R. H.; Dejaegere, A.; Karplus, M. Molecular Mechanics and Dynamics Simulations of Enzymes. *Computational Approaches to Biochemical Reactivity*; Náray-Szabó, G., Warshel, A., Eds.; Kluwer Academic: Boston, 1997; Chapter 4, pp 153−198.
(6) Boyer, P. D. *Angew. Chem., Int. Ed.* **1998**, *37*, 2296−2307.
(7) Walker, J. E. *Angew. Chem., Int. Ed.* **1998**, *37*, 2308−2319.
(8) Uchimaru, T.; Tanabe, K.; Nishikawa, S.; Taira, K. *J. Am. Chem. Soc.* **1991**, *113*, 4351−4353.
(9) Dejaegere, A.; Lim, C.; Karplus, M. *J. Am. Chem. Soc.* **1991**, *113*, 4353−4355.
(10) Lim, C.; Tole, P. *J. Phys. Chem.* **1992**, *96*, 5217−5219.
(11) Tole, P.; Lim, C. *J. Phys. Chem.* **1993**, *97*, 6212−6219.
(12) Tole, P.; Lim, C. *J. Am. Chem. Soc.* **1994**, *116*, 3922−3931.
(13) Dejaegere, A.; Liang, X.; Karplus, M. *J. Chem. Soc., Faraday Trans.* **1994**, *90*, 000.
(14) Chang, N. Y.; Lim, C. *J. Phys. Chem. A* **1997**, *101*, 8706−9713.
(15) Dudev, T.; Lim, C. *J. Am. Chem. Soc.* **1998**, *120*, 4450−4458.
(16) Florián, J.; Warshel, A. *J. Am. Chem. Soc.* **1997**, *119*, 5473−5474.
(17) Florián, J.; Warshel, A. *J. Phys. Chem. B* **1998**, *102*, 719−734.
(18) Holmes, R. R. *Pentacoordinated Phosphorus-Reaction Mechanisms*; ACS Monograph 175; American Chemical Society: Washington, DC, 1980; Vol. I.
(19) Holmes, R. R. *Pentacoordinated Phosphorus-Reaction Mechanisms*; ACS Monograph 176; American Chemical Society: Washington, DC, 1980; Vol. II.
(20) Cramer, C.; Hawkins, C.; Truhlar, D. *J. Chem. Soc., Faraday Trans.* **1994**, *90*, 1802−1804.
(21) Chang, N. Y.; Lim, C. *J. Am. Chem. Soc.* **1998**, *120*, 2156−2167.
(22) Lopez, X; Dejaegere, A.; Karplus, M. Unpublished data.

10.1021/ja010683y CCC: $20.00
Published on Web 11/03/2001

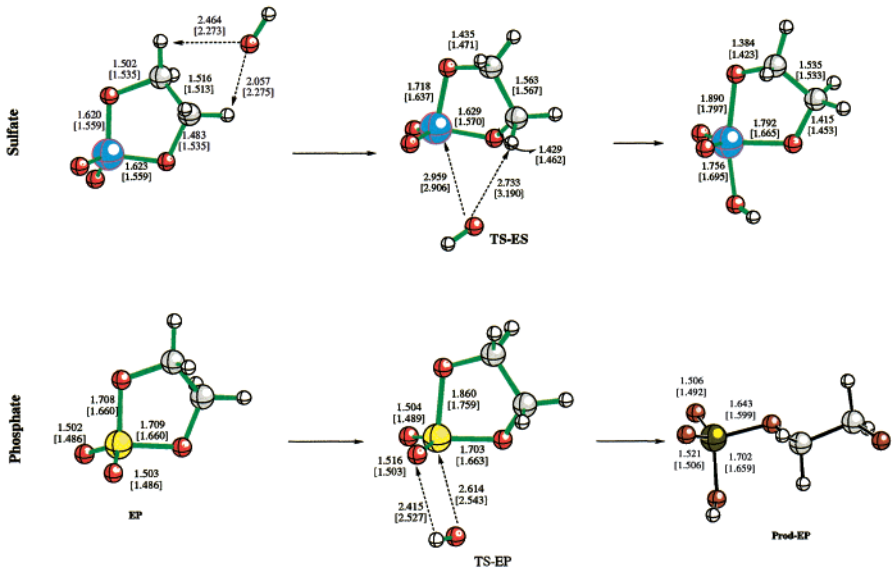

Figure 1. Gas-phase hydrolysis of ethylene sulfate (top) and ethylene phosphate (bottom). For ES, the ion−molecule complex, the transition state, and the intermediate are shown (top). For EP^-, the reactant, the transition state, and the product are shown (bottom). The alkaline hydrolysis of ES involves a pentacovalent intermediate, whereas no stable pentacovalent intermediate could be found for the EP^- reactant. Important distances corresponding to B3LYP/6-31+G* and HF/3-21+G* (in brackets) levels of theory are indicated.

from one system to another. For example, solvation has a rather large effect on the sulfate hydrolysis reaction[4] and a less important one on the phosphate reactions.[22] The effect of solvation was also found to be sensitive to the inclusion of electron correlation; that is, in the hydrolysis of ethylene sulfate, solvation favors a shorter S−OH distance in the TS at the Hartree−Fock level and a longer S−OH distance when using density functional theory at the B3LYP level. In some instances the effects of solvation were found to be in accord with the anti-Hammond postulate rather than the Hammond postulate; that is, in the hydrolysis of dimethyl and ethylene phosphate, solvation favors a more associative transition state with shorter $P-O_{apical}$ bonds, although the solvation free energy of the reaction complexes is larger (in absolute value) for more associative structures.

In this contribution, we reexamine in more detail the potential energy surfaces for the alkaline hydrolysis reaction of sulfates and phosphates, both in the gas phase and in solution. We show that the geometrical distortions caused by the solvent can be understood by application of the Hammond and anti-Hammond postulates. The Hammond postulate states that raising the energy of a structure causes the transition state to resemble that structure, if the energy increases in a direction parallel to the reaction coordinate; the anti-Hammond postulate states that lowering the energy of a structure causes the transition state to resemble that structure, if the energy diminishes in a direction perpendicular to the reaction coordinate.[23−25]

The Hammond and anti-Hammond postulates have been applied most frequently to the analysis of experimental data on the effects of substituents on a reaction. We show that they are useful for interpreting theoretical results concerning solvation. In particular, we identify the variables that dominate the reaction coordinate around the transition state and map the potential energy surface as a function of these variables. From the calculations, we have direct knowledge of the potential energy surface, in contrast with the inferences obtained from experimental data, so that we can determine directly how solvation modifies the surface and the geometries of the various minima and transition states. This makes possible a detailed analysis of how these modifications relate to the Hammond and anti-Hammond effects.[23,25]

We analyze four different reactions: the alkaline hydrolysis of ethylene sulfate (ES) and ethylene phosphate (EP^-), and the alkaline hydrolysis of dimethyl sulfate (DMS) and dimethyl phosphate (DMP^-). We focus primarily on the cyclic systems (ES and EP^-). The acyclic systems (DMS and DMP^-) are then briefly described and compared with the cyclic systems. The cases considered include reactions in which the total charge of the system corresponds to −1 (OH^- + sulfate) and −2 (OH^- + phosphate$^-$). In the former, the solvent disfavors the reaction, whereas in the latter the solvent favors the reaction, as described above. The differences between the cyclic/acyclic cases are of interest, since the geometrical constraints of the former (maintaining the ring) can have consequences for the geometrical distortion of the transition states.

2. Methods

All the structures of Figures 1, 2, and 3 were optimized at HF/3-21+G*[26] and B3LYP/6-31+G(d) levels of theory.[27−31] For the estimation of the change of the geometry in solution the SCI-PCM polarizable continuum model was used. In the PCM methods[32−34] the solute molecule is embedded in a cavity in a dielectric medium which represents the solvent. Solute−solvent interactions are described by a reaction potential arising from the presence of the dielectric medium. The polarization of the solvent is represented by a charge density

(23) Jencks, W. P. *Chem. Rev.* **1985**, *85*, 511−527.
(24) Hammond, G. *J. Am. Chem. Soc.* **1955**, *77*, 334.
(25) Thornton, E. *J. Am. Chem. Soc.* **1967**, *89*, 2915.
(26) Hehre, W.; Radom, L.; Schleyer, P.; Pople, J. *Ab Initio Molecular Orbital Theory*; Wiley-Interscience: New York, 1986.
(27) Becke, A. *Phys. Rev. A* **1988**, *38*, 3098.
(28) Lee, C.; Yang, W.; Parr, R. *Phys. Rev. B* **1988**, *37*, 785.
(29) Vosko, S. H.; Wilk, L.; Nusair, M. *Can. J. Phys.* **1980**, *58*, 1200.
(30) Becke, A. *J. Chem. Phys.* **1993**, *98*, 5648.
(31) Stephens, P.; Devlin, F.; Chabalowski, C.; Frisch, M. *J. Phys. Chem.* **1994**, *98*, 11623−11627.
(32) Cossi, M.; Barone, V.; Cammi, R.; Tomasi, J. *Chem. Phys. Lett.* **1996**, *255*, 327−335.
(33) Mineva, T.; Russo, N.; Sicilia, E. *J. Comput. Chem.* **1998**, *19*, 290−299.
(34) Wiberg, K.; Keith, T.; Frisch, M.; Murcko, M. *J. Phys. Chem.* **1995**, *99*, 9072.

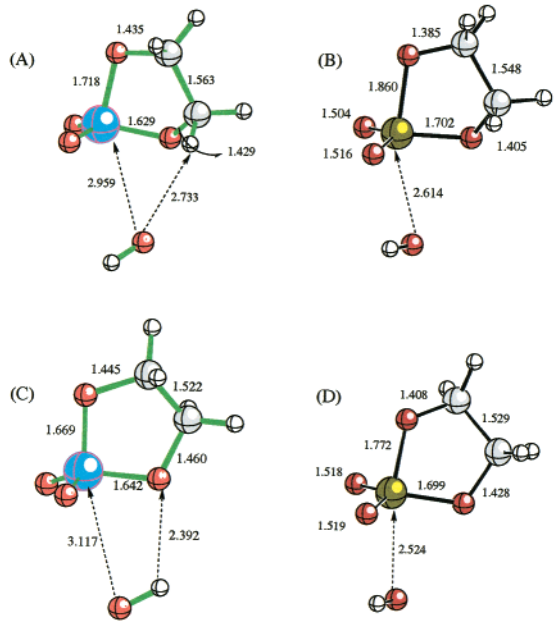

Figure 2. Hydrolysis of ethylene sulfate (ES, left side) and ethylene phosphate (EP^-, right side). Transition states in the gas phase (top) and in solution (bottom), calculated at B3LYP/6-31+G* and B3LYP-(SCI-PCM)/6-31+G* levels of theory, respectively.

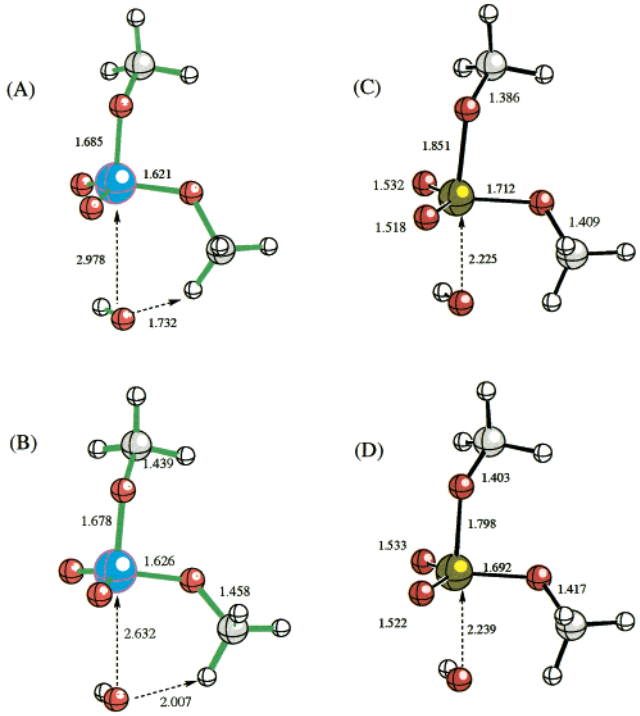

Figure 3. Hydrolysis of dimethyl sulfate (DMS, left side) and dimethyl phosphate (DMP^-, right side). Transition states in the gas phase (top) and in solution (bottom), calculated at B3LYP/6-31+G* and B3LYP-(SCI-PCM)/6-31+G* levels of theory, respectively.

introduced on the surface of the cavity surrounding the solute. The reaction potential $\Phi(r)$ at a point r takes the form

$$\Phi(r) = \int_S \mathrm{d}r^t \frac{\sigma(r^t)}{|r - r^t|} \qquad (1)$$

In the self-consistent isodensity PCM (SCI-PCM) approach,[34] the cavity is derived from an isosurface of the total electron density. All of the optimizations were done using GAUSSIAN 94[35] without charge renormalization since it is not available in the program. The solvation free energies are sensitive to the renormalization of the charge, particularly for small negative ions. In a previous paper on the sulfate hydrolysis reaction,[4] we used SCI-PCM geometries in solution and recomputed the energies at the SCI-PCM geometries with PCM (i.e., the cavity defined by overlapping van der Waals spheres centered on each atom) and including renormalization; we used "method 4" as described in GAUSSIAN 98[36] The results explained the experimental measurements of the difference between cyclic and acyclic sulfate hydrolysis.[4] In the present paper, which is concerned with qualitative trends in the change in geometry, we used the SCI-PCM method without renormalization. To validate the SCI-PCM geometries, classical Poisson calculations and contour plots of the potential energy surface are presented for comparison (see below). The classical Poisson calculations at different points of the gas-phase potential energy surface allow us to predict the distortion expected upon solvation of the system. Since the Poisson equations are solved for a set of partial point charges and explicit electron distribution do not appear, no renormalization is needed. As we demonstrate, there is an excellent agreement between the potential energy surfaces resulting from adding the gas-phase energies to the Poisson solvation free energies (Figure 4C) and the SCI-PCM optimizations for transition-state geometries.

The two-dimensional contour plots obtained with the Poisson equation were used also to obtain insight into the reaction. The two most important internal variables for the description of the reaction coordinate were selected in each case, and the other internal degrees of freedom were fully optimized at HF/3-21+G* level. In the case of the [ES + OH^-] reaction potential energy surface (PES), the variable used were the S−OH distance and the O_{ap}−S−OH angle, and we used a grid of 0.25 Å and 10° for the S−OH distance and the O_{ap}−S−OH angle, respectively. The solvation free energies for some of the gas-phase structures were then evaluated by use of Poisson calculations,[37,38] with the HF/3-21+G* Mulliken atomic charges. A modified version of the UHBD program[39] was employed for these calculations. Poisson calculations were done for a grid of 0.5 Å for the S−OH variable and the following values for the O_{ap}−S−OH angle: 70, 100, 130, 150, 170. For the [EP^- + OH^-] reaction PES, the reaction coordinate was dominated by the P−OH and P−O_{ap} distances, and contour plots for the variation of the HF/3-21+G* electronic energy were calculated in the range 1.8−3.0 Å for the P−OH distance and 1.6−3.8 Å for the P−O_{ap} distance at intervals of 0.2 Å. Poisson calculations were run for all the HF/3-21+G* structures.

3. Results and Discussion

3.1. Hydrolysis of Cyclic Compounds. The alkaline hydrolysis of cyclic ethylene sulfate (ES) and ethylene phosphate (EP^-) has been studied extensively by ab initio methods. We have found that the difference in the total charges of the two reactants leads to important differences in the gas-phase reaction

(35) Frisch, M. J.; Trucks, G. W.; Schlegel, H. B.; Gill, P. M. W.; Johnson, B. G.; Robb, M. A.; Cheeseman, J. R.; Keith, T.; Petersson, G. A.; Montgomery, J. A.; Raghavachari, K.; Al-Laham, M. A.; Zakrzewski, V. G.; Ortiz, J. V.; Foresman, J. B.; Peng, C. Y.; Ayala, P. Y.; Chen, W.; Wong, M. W.; Andres, J. L.; Replogle, E. S.; Gomperts, R.; Martin, R. L.; Fox, D. J.; Binkley, J. S.; Defrees, D. J.; Baker, J.; Stewart, J. P.; Head-Gordon, M.; Gonzalez, C.; Pople, J. A. *Gaussian 94*; Gaussian, Inc.: Pittsburgh, PA, 1995.

(36) Frisch, M. J.; Trucks, G. W.; Schlegel, H. B.; Scuseria, G. E.; Robb, M. A.; Cheeseman, J. R.; Zakrzewski, V. G.; Montgomery, J. A., Jr.; Stratmann, R. E.; Burant, J. C.; Dapprich, S.; Millam, J. M.; Daniels, A. D.; Kudin, K. N.; Strain, M. C.; O. Farkas, J. T.; Barone, V.; Cossi, M.; Cammi, R.; Mennucci, B.; Pomelli, C.; Adamo, C.; Clifford, S.; Ochterski, J.; Petersson, G. A.; Ayala, P. Y.; Cui, Q.; Morokuma, K.; Malick, D. K.; Rabuck, A. D.; Raghavachari, K.; Foresman, J. B.; Cioslowski, J.; Ortiz, J. V.; Stefanov, B. B.; Liu, G.; Liashenko, A.; Piskorz, P.; Komaromi, I.; Gomperts, R.; Martin, R. L.; Fox, D. J.; Keith, T.; Al-Laham, M. A.; Peng, C. Y.; Nanayakkara, A.; Gonzalez, C.; Challacombe, M.; Gill, P. M. W.; Johnson, B. G.; Chen, W.; Wong, M. W.; Andres, J. L.; Head-Gordon, M.; Replogle, E. S.; Pople, J. A. *Gaussian 98*, revision A.2; Gaussian, Inc.: Pittsburgh, PA, 1998.

(37) Bashford, D.; Karplus, M. *Biochemistry* **1990**, *29*, 10219.

(38) Lim, C.; Bashford, D.; Karplus, M. *J. Phys. Chem.* **1991**, *95*, 5610.

(39) Davis, M.; Madura, J.; Luty, B.; McCammon, J. *Comput. Phys. Commun.* **1991**, *62*, 187.

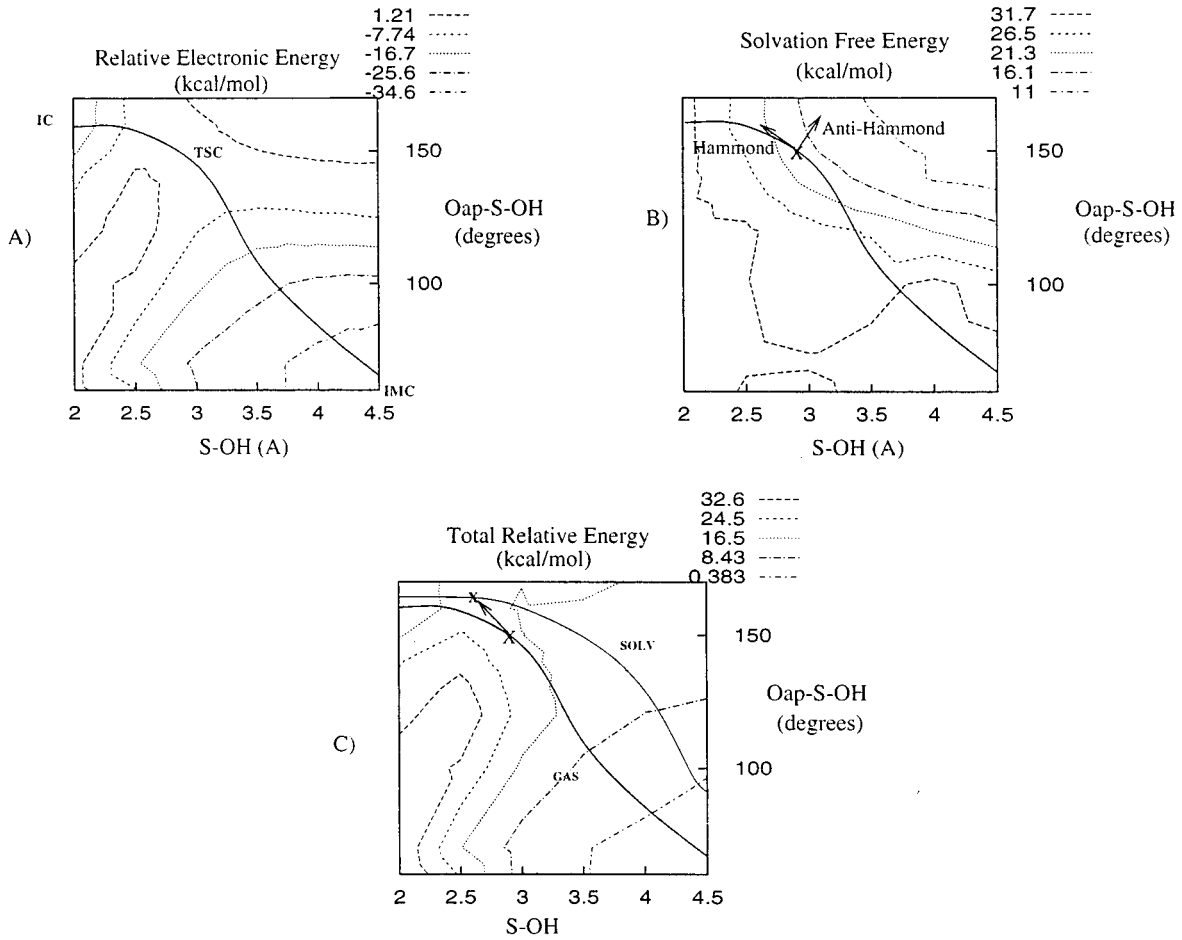

Figure 4. Reaction surfaces (in kcal/mol) for ethylene sulfate as a function of the S−OH and O_{ap}−S−OH internal coordinates. For a definition of these variables see Figure 1. (A) HF/3-21+G* gas-phase electronic energy, (B) Poisson solvation energy, (C) total energy in solution obtained by summing gas phase and Poisson contributions. All values are relative to the ES + OH^- reactants. Solid lines are the gas-phase reaction coordinate in (A) and the solution reaction coordinate (C). The X in (B) and (C) indicates the transition states.

paths. For sulfate, a neutral dipolar reactant, and the negatively charged hydroxyl ion, a very stable ion−dipolar complex is formed prior to the attack of the hydroxyl on the sulfur atom. In the case of ethylene phosphate, by contrast, no ion−molecule complex is formed because of the large repulsions between the negative charges of the hydroxyl anion and the ethylene phosphate anion. This difference in the charge of the ES and EP reactants is also the cause of a substantially different solvent effect on the reaction barriers. For the hydrolysis of ES, the solvent raises the activation barrier with respect to gas phase, since the delocalization of the negative charge of the hydroxyl anion as it approaches the neutral ES reactant results in smaller solvation free energies. By contrast, solvent reduces the gas-phase barriers for the hydrolysis of EP^-, since the solvation free energy depends quadratically on the total charge of the system, so that the transition state (charge of −2) has a larger solvation energy than the sum of the solvation free energies of the reactants (each with charge −1). The resulting solution free energy barrier for hydrolysis of cyclic ES and EP^- are quite similar (29.6 kcal/mol for EP^{-9} and 17.2 kcal/mol for ES,[4] in contrast to the gas-phase values of 85.0 kcal/mol for EP^{-9} and 4.8 kcal/mol for ES[4]). The distortion induced in the gas-phase transition-state geometry by the solvent is very different in the two cases. Whereas solvent increases the S−OH distance at the transition state for ethylene sulfate, in the case of EP^-, it shortens the P−OH distance significantly. To interpret the difference in the solvent effect for the two systems, we use the Hammond and anti-Hammond postulates.

3.1.1. Hydrolysis of Ethylene Sulfate. When the OH^- group approaches ES in the gas phase, a very stable ion−molecule complex is formed (Figure 1a). The rate-limiting step of the reaction corresponds to the transition from this ion−molecule complex to the pentacovalent sulforane intermediate (Figure 1c) through the transition state TS-ES (Figure 1b).The second step of the reaction is the breaking of the $S-O_{axial}$ endocyclic bond and formation of a sulfate product. The transition states and barriers for this second step have been estimated by Cameron et al.,[3] and they are lower than those of the first step of the reaction. For more details on this reaction, we refer the reader to refs 2−4.

To pass from the ion−molecule complex to the pentacovalent intermediate, two major geometrical changes have to take place: There is a shortening of the S−OH distance (from 4.85 to 1.70 Å at HF/3-21+G*) and an increase of the O_{ap}−S−OH angle (from 48.3° to 167.7° at HF/3-21+G*) (see Table 1). The reaction coordinate is expected to have large contributions from both of these coordinates. To obtain a more quantitative description of the reaction, we determined the gas-phase HF/3-21+G* potential energy surface as a function of the reaction coordinates: the S−OH distance and the O_{ap}−S−OH angle (see Methods). These data are presented in Figure 4A. The reaction coordinate (i.e., the minimum-energy path connecting the ion−molecule complex and the pentacovalent intermediate) inferred from the surface is indicated in the figure. At long S−OH distances (>4.0 Å), the S−OH distance dominates the reaction coordinate, but as the reaction proceeds toward the transition

Table 1. Hydrolysis of ES and DMS Sulfates; S−OH (Å) and O_{ap}−S−OH (deg) for the Ion−Molecule Complexes, Transition States, and Intermediates

	ion−molecule		transition state		intermediate	
theory	S−O_H	∠$O_{ap}SO_H$	S−O_H	∠$O_{ap}SO_H$	S−O_H	∠$O_{ap}SO_H$
Cyclic Ethylene Sulfate						
HF/3-21+G*	4.85	48.3	2.91	147.9	1.70	167.7
HF(SCIPCM)			2.68	167.0		
B3LYP/6-31+G*	4.93	45.5	2.96	138.7	1.76	164.7
B3(SCIPCM)			3.12	162.8	1.76	166.2
Acyclic Dimethyl Sulfate						
B3LYP/6-31+G*	4.35	59.4	2.98	172.7	1.82	170.8
B3(SCIPCM)			2.64	174.5	1.81	170.8

state, the OH^- group rotates to a position closer to in-line attack, and the reaction coordinate therefore has a large angular O_{ap}−S−OH component (in the region (3−4 Å) for the S−OH distance). At short S−OH bond-distances, the reaction coordinate corresponds again mainly to S−OH elongation, with a small, but nonnegligible, contribution from the O_{ap}−S−OH angle. Thus, both the S−OH and O_{ap}−S−OH coordinates are involved in the reaction coordinate, but to a different degree as the reaction proceeds. The transition state in the gas phase is located at a S−OH distance of 2.91 Å and an O_{ap}−S−OH angle of 147.9°.

To determine the effect of solvation on the reaction, we did a HF(SCI-PCM)/3-21+G* optimization of the transition state (see Methods). The solvent is found to favor a more associative and *in-line* mechanism. The S−OH distance shortened to 2.68 from 2.91 Å, and the angle was increased to 167.0° from 147.9°. To interpret the changes in the reaction coordinate with solvation, we calculate the solvation contribution to the potential energy surface using the same structures as for the gas-phase surface and Poisson calculations (see Methods). The results are shown in Figure 4B. The numbers in the figure correspond to solvation free energies relative to those of the reactants. Since solvation raises the activation barrier (i.e., the reactants are better solvated than the reaction complexes), the relative solvation values are all positive. Smaller numbers therefore indicate better solvation and lower activation barriers.

The best solvated structures are those with long S−OH distances and large O_{ap}−S−OH angles, for which the hydroxyl group is less shielded by the sulfate group. Figure 4C shows the solvated potential energy surface relative to the reactants (gas-phase quantum-mechanical plus classical solvation contribution) and the minimum energy path in solution, as well as in the gas phase for comparison. It can be seen that in solution the reaction coordinate is modified in such a way that an "in-line"attack (i.e., large O_{ap}−S−OH angles) is maintained for a greater range of S−OH distances. On this potential surface, the transition state is located at 2.59 Å for S−OH and 163.5° for O_{ap}−S−OH. This is in reasonable agreement with the geometry found by full optimization in solution using the HF(SCI-PCM) method without renormalization (see Methods) (2.68 Å for S−OH and 167.0° for O_{ap}−S−OH). The classical Poisson solvation contribution thus predicts correctly the direction of the geometrical distortion: solvation favors a more associative transition state with a more *in−line* mechanism, in agreement with the HF(SCI-PCM) results. Moreover, since the largest error in the SCI-PCM calculations without renormalization[4] arises from the too-small energy calculated for OH^-, optimization with a renormalized energy is expected to shift the geometry further in the direction found with the unnormalized calculation, that is, even closer to the Poisson results.

We can thus use the Poisson potential surface (Figure 4B) to interpret the geometrical effects of solvation by the Hammond and anti-Hammond postulates, which are concerned with the transition-state behavior parallel and perpendicular to the reaction coordinate, respectively; see arrows in Figure 4B. In accord with the Hammond postulate, an effect that raises the energy of a structure causes the transition state to have greater resemblance to that structure. This means that in the Hammond direction the distortion of the transition state by solvent, relative to the gas phase, will be dictated by the direction in which the solvation free energy is more positive relative to the reactants, since as discussed above, the solvent *destabilizes* the transition state. The result is shown by the Hammond arrow in Figure 4B. The S−OH distance becomes shorter, and the O_{ap}−S−OH angle, larger, both of which decrease the magnitude of the total solvation free energy. By the anti-Hammond postulate the converse is expected for directions perpendicular to the reaction coordinate; that is the transition state is distorted to achieve a larger solvation free energy, which leads to longer S−OH distances and larger O_{ap}−S−OH angles; this is indicated by the anti-Hammond arrow in Figure 4B.

In summary, both the Hammond and anti-Hammond effects favor an *in-line* mechanism. However, the Hammond effect leads to a shortening of the S−OH distance, whereas the anti-Hammond effects favors a lengthening of the S−OH distance. Which of the effects is dominant for the S−OH distance depends on its contribution to the Hammond and anti-Hammond vectors. For the HF/3-21+G* level of theory at the gas-phase transition state, the S−OH distance is the major component of the reaction coordinate, and therefore, the Hammond effect is dominant in the distortion of S−OH. This corresponds to the calculated shortening of the S−OH distance when the transition state is optimized in solution with HF(SCI-PCM)/3-21+G* method, in correspondence with the Poisson calculations and the two-dimensional contour plots.

Effect of Correlation. To determine the effect of the electron correlation on the reaction coordinate, we compare the results obtained with HF and B3LYP levels of theory (see Methods). In the gas phase, the HF/3-21+G* and B3LYP/6-31+G* transition states have similar structures. However, when the transition state is optimized in solution using the B3LYP(SCI-PCM)/6-31+G* method, the transition state is shifted to *longer* S−OH distances and larger angles; that is S−OH is equal to 3.12 Å (2.96 Å in the gas phase) and O_{ap}−S−OH is equal to 162.8° (138.7° in the gas phase). To explain this difference between the HF and B3LYP calculations, it is useful to look again at the reaction coordinate. Recently, we have determined the B3LYP/6-31+G* gas-phase intrinsic reaction coordinate[40,41] (IRC) for the hydrolysis of ES. In Figure 5A we show again the HF two-dimensional contour plot for the gas-phase energy, along with the reaction path and the Hammond analysis vectors from Figure 4B. Figure 5B depicts the values of S−OH and O_{ap}−S−OH for each of the IRC-optimized structures calculated in ref 4. With B3LYP/6-31+G*, the reaction coordinate from the reactant to the TS shows a larger contribution from the O_{ap}−S−OH angle, relative to the S−OH distance, than in the HF case. Correspondingly, the transition state has a smaller O_{ap}−S−OH angle, 138.7°, than at HF/3-21+G* (O_{ap}−S−OH is 147.9°), whereas the S−OH distance is essentially the same (2.96 Å at B3LYP/6-31+G* and 2.91 Å at HF/3-21+G*). The larger coupling of S−OH and O_{ap}−S−OH has an important influence on the change of S−OH distance upon solvation.

(40) Gonzalez, C.; Schlegel, B. *J. Chem. Phys.* **1989**, *90*, 2154.
(41) Gonzalez, C.; Schlegel, B. *J. Phys. Chem.* **1990**, *94*, 5523−5527.

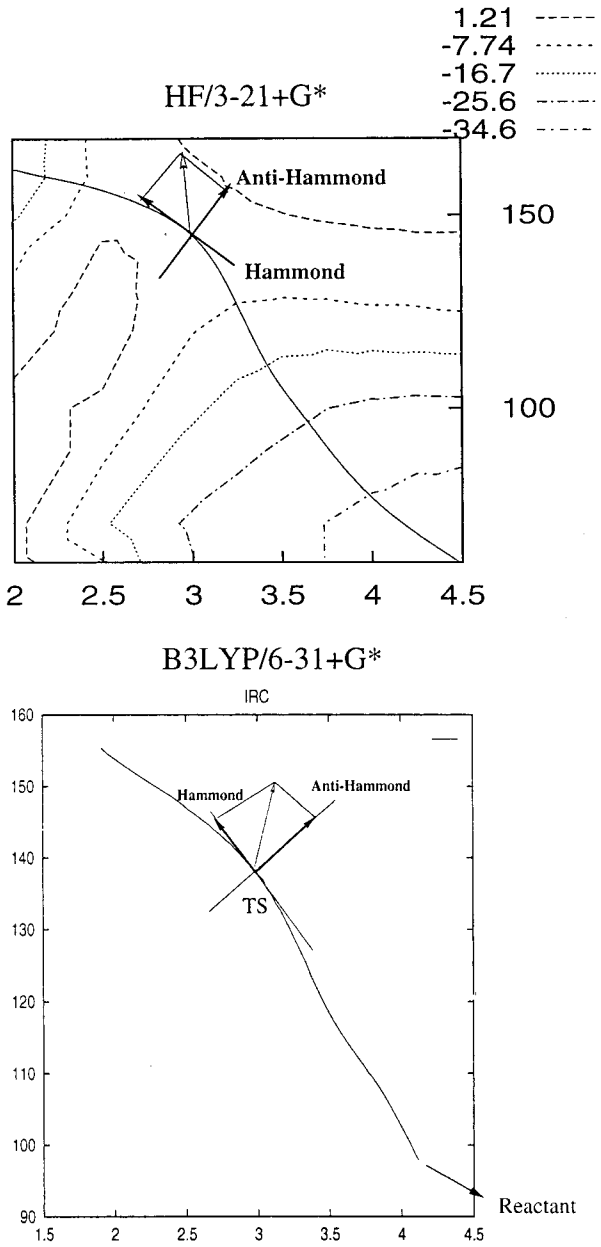

Figure 5. Hammond and anti-Hammond effects on the HF/3-21+G* (top) and B3LYP/6-31+G* (bottom) reaction coordinates. To obtain the B3LYP/6-31+G* reaction coordinate we have taken the S−OH distance and O_{ap}−S−OH angle values from each of the IRC-optimized geometries. The contour plot of the top figure corresponds to the gas-phase potential energy surface at HF/3-21+G* level of theory.

Although we did not determine a solvated free energy surface in this case, we determined the transition state in solution using the B3LYP(SCI-PCM)/6-31+G* level of theory.

The arrows in Figure 5B correspond to the distortion one finds in the TS going from the gas phase (B3LYP calculations) to the solvent (B3LYP(SCI-PCM)). With respect to the HF data, there is an increase of the S−OH component in the anti-Hammond vector and a concomitant decrease of the S−OH component in the Hammond vector. The components are such that the changes in S−OH distance is dominated by the anti-Hammond effect, so that a larger S−OH distance results. Thus, at correlated levels of theory, both the O_{ap}−S−OH angle and the S−OH distance are increased by solvation. This leads to a more dissociative mechanism.

The comparison between uncorrelated and correlated results shows that, in the former, solvation tends to favor a more associative transition state than in the gas phase, whereas the reverse is true for the latter. The degree of S−OH, O_{ap}−S−OH coupling in the reaction coordinate and the Hammond and anti-Hammond effects determines the changes in S−OH of the transition state upon solvation. Both correlated and uncorrelated levels favor a more *in-line* mechanism with solvation. That correlation effects can be important for determining the associative versus dissociative character for a reaction is an important result that could be of more general significance. However, as Lynch et al.[42] have pointed out recently, B3LYP appears to systematically underestimate barrier heights. This would be likely to lead to some errors in the transition state geometries. Thus, the true situation is likely to be somewhere between the HF and B3LYP results.

Table 2. Hydrolysis of EP^- and DMP^- Phosphates; P−OH and P−O_{ap} Distances (Å), and $O_{ap}PO_H$ Angle (deg) at the Cyclic and Acyclic Transition States

theory	transition state		
	P−O_H	P−O_{ap}	∠$O_{ap}PO_H$
Cyclic Ethylene Phosphate			
HF/3-21+G*	2.54	1.76	164.4
HF(SCIPCM)	2.43	1.72	167.4
B3LYP/6-31+G*	2.61	1.86	164.1
B3(SCIPCM)	2.52	1.77	165.5
Acyclic Dimethyl Phosphate			
B3LYP/6-31+G*	2.23	1.85	171.0
B3(SCIPCM)	2.24	1.80	173.3

3.1.2. Hydrolysis of Ethylene Phosphate (EP^-). The alkaline hydrolysis of ethylene phosphate (EP^-) involves the approach of two negative charges. In a vacuum, the two groups with a negative charge strongly repel each other, and the activation barrier is very large (on the order of 85−95 kcal/mol[9]). Moreover, the resulting phosphorane intermediates are unstable. Attempts to optimize such a pentacovalent structure leads to the breaking of the P−O_{ap} axial bond and opening of the ring. Thus, the hydrolysis of EP^- is a one-step process, with no stable pentacovalent intermediates (see Figure 1b).

The transition-state structure (TS-EP) for hydroxyl attack on ethylene phosphate is shown in Figure 2. The most important geometrical parameters are given in Table 2. At the HF/3-21+G* level of theory, the P−OH and P−O_{ap} distances are 2.54 and 1.76 Å, respectively, and electron correlation lengthens these distances to 2.61 and 1.86 Å, respectively. There is an essentially *in-line* attack, which is almost invariant to the theoretical level (164.4° at HF and 164.1° at B3LYP).

When the transition states are optimized in solution (see Methods and description of the ethylene sulfate results), there is a shortening of both the P−OH and P−O_{ap} distances. At HF-(SCI-PCM) we find values of 2.43 and 1.72 Å for P−OH and P−O_{ap}, respectively. When the SCI-PCM optimizations are done using the B3LYP/6-31+G* method, we also get a shortening of the P−OH and P−O_{ap} distances to 2.52 and 1.77 Å, respectively. Thus, there is no qualitative difference between correlated and uncorrelated results. The O_{ap}−P−OH angle changes little upon solvation; that is the values are 164.1° (gas phase) and 165.5° (solution) at B3LYP/6-31+G* level of theory. Thus, the solvent distorts the transition state to more associative geometries, with a decrease of about 0.1 Å for both P−OH and P−O_{ap} distances, and little change in the O_{ap}−P−OH angle, which is already quite open in the gas phase.

To understand why the solvent favors a more associative mechanism for EP^- (i.e., shorter P−OH and P−O_{ap}), we

(42) Lynch, B. J.; Fast, P. L.; Harris, M.; Truhlar, D. G. *J. Phys. Chem. A* **2000**, *104*, 4811−4815.

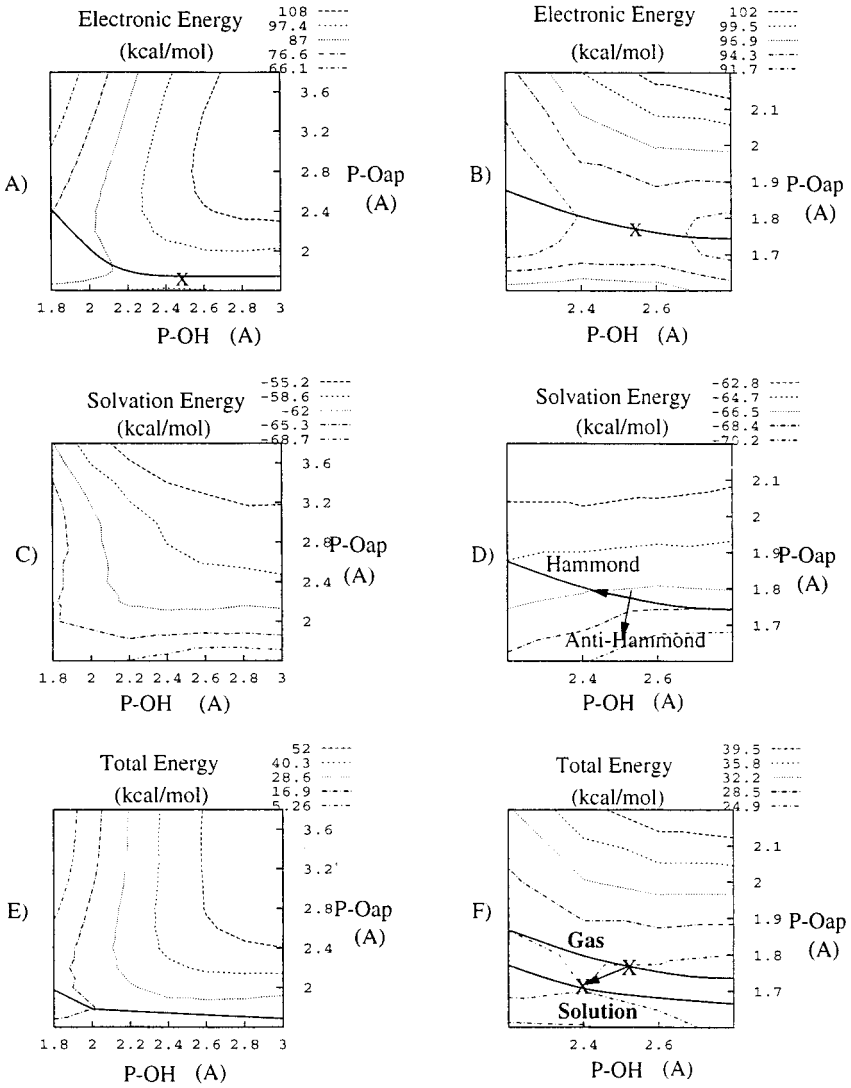

Figure 6. Reaction surface of ethylene phosphate. (A) and (B) HF/3-21+G* gas-phase electronic energy; (C) and (D) Poisson solvation free energies; (E) and (F) total energies obtained from summation of the gas phase and solvation free energies. All values are relative to the $EP^- + OH^-$ reactants. Solid lines are the gas-phase reaction coordinate in (A), (B), and (D). Both the gas-phase and solution reaction coordinate are shown in (F). The X in (A) and (F) indicates the transition states. The energies for the whole range of P−OH and P−O_{ap} distances are shown on the left-hand side (A, C, E) diagrams. The region around the transition state is shown in the right-hand side (B, D, F) diagrams.

calculated contour plots of the HF/3-21+G* energy with respect to the P−OH and P−O_{ap} distances. These are the appropriate variables for this case because there is only a small change in O_{ap}−P−OH angle as a function of the level of theory and with solvation. The contour plots are shown in Figure 6; they cover a range of 1.8−3.0 Å for P−OH and 1.6−3.8 Å for P−O_{ap}. As for ES, the gas-phase electronic energies, solvation free energies from Poisson calculations, and the total energies, which give an approximation to the reaction path in solution, are given. Energies relative to the reactants are shown. The energies for the whole range of P−OH and P−O_{ap} distances are shown on the left-hand side (A, C, E) diagrams of Figure 6, and the region around the transition state is shown on the right-hand side (B, D, F).

The reaction coordinate in the gas phase (Figure 6, A and B) corresponds almost exclusively to the variation of the P−OH distance for large values of P−OH (>2.3 Å). Only for P−OH below 2.2 Å is there a significant contribution from the P−O_{ap} elongation. Contrary to the sulfate case, solvation free energies are always larger in absolute value for the EP−OH structures than for the reactants. That is why in Figure 6, C and D we obtain negative numbers for the relative solvation free energies with respect to the reactants. A larger negative number implies better solvation. In general, the solvation free energies are larger (more negative) for short P−OH and P−O_{ap} distances (see Figure 6C), because at long P−OH and P−O_{ap} distances there is a greater separation of the negative charges. Since the solvation free energy varies with the square of the charge (Born model), one expects that separation of the charges leads to smaller solvation free energies. However, there are some local deviations from this general behavior. At short P−O_{ap} distances, in the region around the transition state (see Figure 6D), the solvation free energy is only weakly dependent on the P−OH distance, that is, the contour lines are almost parallel to the P−OH axis, and the changes in solvation free energy are related primarily to the variations in P−O_{ap}.

The gas-phase and solvation reaction paths estimates are shown in Figure 6, E and F, which give the total energy (HF/3-21+G* plus classical Poisson) in solution.

It can be seen from Figure 6F that the solvation reaction path and transition state have a more associative character than in the gas phase, in agreement with the geometry optimizations using the SCI-PCM method. To interpret the geometrical distortion introduced by solvation, we use the Hammond and

anti-Hammond postulates, as depicted in Figure 6D. The Hammond vector is parallel to the reaction coordinate and points in the direction of increasing energy, which on Figure 6D corresponds to shorter P−OH and longer P−O_{ap}. The anti-Hammond vector is perpendicular to the reaction coordinate and points in the direction of decreasing energy, which from Figure D corresponds to shorter P−OH and shorter P−O_{ap}. For the changes in the P−OH distance, both effects are in the same direction, while the two effects are in opposite directions for the P−O_{ap} distance. The geometrical changes in solvation are toward shorter P−OH and shorter P−O_{ap} (cf. Figure 6F), which indicates that the anti-Hammond effect dominates the distortion of P−O_{ap}.

Overall, the geometrical changes induced by the solvent in EP^- are significantly smaller than for the sulfate case, in accord with the estimates of solvent distortions in MEP, TMP, and MPP reported by Lim et al.[21] The magnitude of the geometrical distortion induced by solvation depends both on the shape of the gas-phase potential energy surface and on the shape of the "solvation surface". For example, the change in solvation free energies in the Hammond directions (toward shorter P−OH distances) are very small (cf. Figure 6D) so that change in geometries due to the Hammond effect would also be expected to be small. However, in that direction the gas-phase potential energy surface is very flat (cf. Figure 6B), so that small geometrical distortions around the gas-phase TS are easy to achieve and therefore a small distortion (0.1 Å) is observed for the P−OH distance. In the anti-Hammond direction, the variations of solvation free energies are more significant (cf. Figure 6D). However the gas phase surface is also considerably steeper (cf. Figure 6B), and thus geometrical distortion is more difficult to achieve. Hence, there is also only a small geometrical change in the anti-Hammond direction P−O_{ap}, as well (0.1 Å).

3.2. Hydrolysis of Acyclic Compounds. Solvation also alters the geometries of the transition state for the hydrolysis of acyclic sulfates (DMS) and phosphates (DMP^-). Interestingly, in the case of dimethyl sulfate, the effect using the correlated B3LYP-(SCI-PCM) method is opposite to the one found for its cyclic counterpart, that is, the transition state for the hydrolysis of DMS becomes more associative in the presence of solvent. For the hydrolysis of dimethyl phosphate the transition state is only slightly distorted. These effects can be understood using the information from the 2D-diagrams of the cyclic compounds, ES and EP^-.

3.2.1. Dimethyl Sulfate (DMS). The rate-limiting transition state TS-DMS for the hydrolysis of dimethyl sulfate is depicted in Figure 3. The values for the S−OH and O_{ap}−S−OH internal coordinates are listed in Table 1. The reaction is similar to the cyclic case, in that the rate-limiting step in the gas phase is the passage from the acyclic ion−molecule complex to the acyclic intermediate. The cyclic/acyclic ion−molecule complexes and intermediates show certain similarities; in particular, the acyclic transition state is also early with a long S−OH distance. However, there is an important difference between the acyclic and cyclic transition states. The O_{ap}−S−OH angle in the former is 172.7°, much larger than the O_{ap}−S−OH angle in the cyclic case (138.7°). This implies that the gas-phase transition state in the acyclic reaction is located in a region where the reaction coordinate is dominated by the elongation of the S−OH bond. Consequently, the Hammond postulate for motion along the reaction coordinate can be used to understand the change of the S−OH distance by the solvent. Since larger solvation free energies (smaller positive values in the 4B diagram) are obtained for longer S−OH distances, the transition state is expected to have a shorter S−OH distance. This is in accord with the B3LYP(SCI-PCM)/6-31+G* optimized transition state, which has a S−OH distance of 2.64 Å, around 0.3 Å shorter than in the gas phase.

3.2.2. Dimethyl Phosphate (DMP^-). The transition states for hydroxyl attack on dimethyl phosphate in the gas phase and in solution are shown in Figure 3. The P−OH distance equals to 2.23 Å at the B3LYP/6-31+G* level of theory. This is much shorter than that of the cyclic analogue (2.64 Å) and also significantly shorter than the S−OH distance (2.98 Å) found for the attack of the hydroxyl on the acyclic DMS sulfate. The effect of the solvent on the transition-state geometries are shown in Figure 3 and Table 2. The P−O_{ap} distance is shortened to 1.80 Å (from 1.85 Å in the gas phase). However, the P−OH distance is almost invariant; it is lengthened by only 0.01 Å. This small change in P−OH distance is consistent with the small variation of the solvation free energies with P−OH found for the cyclic ethylene phosphate.

4. Conclusions

We have studied the effect of solvent on the geometries for the rate-limiting transition states of the hydrolysis reactions of cyclic and acyclic phosphate and sulfate esters. Application of the Hammond and anti-Hammond postulates provides an interpretation of the trends observed for the geometrical distortion of the transition states in solution, relative to the gas phase. The trends observed can be summarized as follows:

(1) For the hydrolysis of EP^- and DMP^-, where the system can be described as the approach of two negative charges, the solvation energy is more negative for associative structures. In the case of ES and DMS, where one negative charge is approaching a neutral system, the solvation energy is more negative for more open structures.

(2) The solvation free energies are larger (in absolute value) for in-line structures. The reason is that the attacking hydroxyl group is less shielded from solvent by the aliphatic hydrogens as the $\angle O_{ap}XO$ (X = P, S) approaches 180°.

(3) The distortion of the geometries of the transition states is interpreted by applying the Hammond and anti-Hammond postulates parallel and perpendicular to the reaction coordinate, respectively.

(i) Regarding the distortion of the X−OH distance in the transition state, both Hammond and anti-Hammond postulates imply a shortening of the P−OH distance, and a more associative transition state in solution than in the gas phase, for the hydrolysis of ethylene phosphate and dimethyl phosphate. The Hammond effect implies a lengthening of the P−O_{ap} distance upon solvation while the solvation free energy increases (in absolute value) for more compact structures. The behavior can be understood by a more detailed examination of the solvated potential energy surface in the region of the transition state; the P−O_{ap} bond obeys the anti-Hammond postulate. In the case of sulfates, the Hammond and anti-Hammond vectors point in different directions for the S−OH distortion. Whereas the Hammond vector favors a shortening of the S−OH distance, the anti-Hammond vector favors an elongation. Which has the dominant effect on the distortion of the S−OH distance upon solvation depends on the degree of coupling between internal coordinates (primarily S−OH and O_{ap}−S−OH) in the reaction coordinate at the transition state.

(ii) With respect to the in-line character of the transition state (i.e., O_{ap}−X−OH angle), both Hammond and anti-Hammond vectors point toward increasing the O_{ap}−X−OH angle, and the inclusion of solvent in the calculations enhances the in-line character of the transition state.

Acknowledgment. The laboratory at the Université Louis Pasteur is supported in part by CNRS (ISIS-UPRES A 7006), by the Ministere de l'EducationNationale. X.L. thanks the CEE for a grant. We thank Professor W. Graham Richards and his group at the Oxford Centre for Molecular Science for their kind hospitality, and Dr. A. Dinner for useful discussions. We also thank the Institut de Development et des Ressources en Informatique Scientifique (IDRIS) for computer time and assistance in this work. The work done at Harvard was supported in part by a Grant from the National Institutes of Health.

JA010683Y